Microplate
Easter island
Plate kinematics
Rapanui expedition
Ridge tectonics

Microplaque
Ile de Pâques
Cinématique des plaques
Expédition Rapanui
Tectonique des dorsales

A tectonic test of instantaneous kinematics of the Easter microplate

Janet H. ZUKIN, Jean FRANCHETEAU

Institut de Physique du Globe, 4 Place Jussieu, 75252 Paris Cedex 05, France.

Received 03/11/89, in revised form 09/04/90, accepted 10/05/90.

ABSTRACT

Detailed studies of the Easter microplate, and other contemporary microplates located along the world's mid-oceanic ridge system, are considered of primary importance to our understanding of the kinematic evolution of the major oceanic plates. The focus of the Rapanui expedition, part of the "Tour du monde" of the French research vessel *Jean Charcot*, was to collect detailed structural and geophysical data along the northern and southern Easter microplate boundaries in order to test, in a rigorous manner, the most recent tectonic and kinematic models for the microplate. In developing detailed bathymetric, morphotectonic and magnetic maps of these boundaries, we have found that our new plate boundaries differ considerably from those of Hey *et al.* (1985). These new boundaries are characterized by complex deformational structures, particularly at the northern and southern triple junctions. The northern boundary is dominated by compression and right lateral shear, particularly to the west, and leads to extension in the east. The southern boundary is dominated by extension, particularly to the west, leading to right lateral shear and compression to the east. We have utilized our detailed data to test Naar and Hey's (1989) instantaneous Euler poles for the Nazca-Easter and Pacific-Easter plate pairs in both a qualitative and quantitative sense, first by comparing the locations of differing deformational regimes (predicted by the Euler pole locations and the locations of the limits between these regimes) with our new plate boundary configurations, and secondly, by making precise comparisons between our profiles and magnetic models which we calculated using the pole locations and angular rotations. We have found that our data agree fairly well with the Nazca-Easter and Pacific-Easter instantaneous Euler pole positions. We have also tested the kinematic microplate models of Engeln *et al.* (1988) and Schouten *et al.* (1988a, 1988b), and have shown that our data are in general agreement with their model of rigid plate rotation, but not with their model of simple shear.

Oceanologica Acta, 1990, volume spécial **10**, Actes du colloque Tour du Monde Jean Charcot, 2-3 mars 1989, Paris. 000-000.

RÉSUMÉ

Test tectonique de la cinématique instantanée de la microplaque de l'île de Pâques

Les études détaillées de la microplaque de l'île de Pâques, et d'autres microplaques présentes le long du système des dorsales médio-océaniques sont essentielles pour comprendre l'évolution cinématique des plaques océaniques majeures. L'objectif principal de l'expédition Rapanui, dans le cadre du Tour du Monde du N/O Jean Charcot était d'acquérir des données structurales et géophysiques détaillées le long des frontières Nord et Sud de la microplaque de l'île de Pâques afin de tester les modèles cinématiques et tectoniques les plus récents de la microplaque. La cartographie bathymétrique,

morphotectonique et magnétique a montré que les frontières de la microplaque diffèrent beaucoup de celles proposées par Hey *et al.* (1985). Ces frontières nouvellement définies sont marquées par des structures à déformation complexe, en particulier aux points triples Nord et Sud de la microplaque. La frontière Nord est caractérisée par une compression et un cisaillement dextré, surtout à l'Ouest, qui passe à une extension à l'Est. La frontière Sud est caractérisée par une extension, surtout à l'Ouest, qui passe à un cisaillement dextre et une compression à l'Est. Les données détaillées ont permis de tester les pôles d'Euler instantanés du modèle de Naar et Hey (1989) pour les mouvements Nazca-Pâques et Pacifique-Pâques sur le plan qualitatif et quantitif d'abord en comparant les domaines des différents régimes de déformation (prédits par les pôles d'Euler) le long des nouvelles frontières et ensuite en comparant les profils magnétiques aux profils synthétiques prédits par les paramètres de rotation. Les données sont en accord raisonnable avec les pôles eulériens instantanés qui décrivent les mouvements relatifs Nazca-Pacifique et Pacifique-Pâques. Nous avons également testé les modèles cinématiques de microplaque d'Engeln *et al.* (1988) et Schouten *et al.* (1988a, 1988b) et montrons que les données sont en accord avec leur modèle de rotation de plaques rigides mais en désaccord avec leur modèle de cisaillement simple.

Oceanologica Acta, 1990, volume spécial **10**, Actes du colloque Tour du Monde Jean Charcot, 2-3 mars 1989, Paris. 000-000.

INTRODUCTION

During the last decade of research over the world's mid-ocean ridge system, scientists have come to realize that this system is made up of a series of complex overlapping rift discontinuities. The largest of these, microplates, have been identified both along the contemporary mid-ocean ridge system as well as found "frozen" into the old ocean basins (Mammerickx *et al.*, 1988) and are thought to play a primary role in the kinematic reorganization of major oceanic plates. Studies which focus on the kinematic evolution of these microplates are therefore considered important to our understanding of the more general evolution of the major oceanic plates, and perhaps to the geodynamic processes controlling this evolution.

The Easter microplate, located between 22°S and 28°S along the East Pacific Rise (EPR) (Fig. 1), is the best known of the contemporary mid-ocean ridge microplates. The majority of studies here have been reconnaissance in nature and have focused on redefining the microplate boundaries (Herron 1972, Forsyth 1972, Anderson *et al.* 1974, Handschumacher *et al.* 1981, Engeln and Stein 1984, Engeln 1985, and Hey *et al.*, 1985). Other studies have focused on the kinematic evolution of the microplate, some by inverting instantaneous Euler poles of rotation for the Pacific-Easter, Nazca-Easter, and Nazca-Pacific plate pairs (Engeln and Stein 1984; Naar and Hey, 1989), and others by producing rigid and shear behaviour models for microplates in general, and the Easter microplate in particular (Engeln *et al.* 1988; Schouten *et al.* 1988). More recent expeditions to this area have resulted in an almost total side-scan sonar insonification of the microplate boundaries and interior (Hey and Naar, 1987; Searle *et al.*, 1989).

The focus of the Rapanui expedition, which took place in early 1987 and was part of the "Tour du Monde" of the French research vessel N/O *Jean Charcot*, was to collect detailed structural and geophysical data along the northern and southern Easter microplate boundaries; these areas are depicted as areas 1 and 2 in Figure 1. With these detailed data (comprising Seabeam swath bathymetry (Renard and Allenou, 1979), magnetics and gravity) we aimed to test, in a rigorous way, the previous plate boundary configuration (Hey *et al.*, 1985) and the most recent kinematic models for the microplate (Naar and Hey, 1989; Engeln *et al.*, 1988; Schouten *et al.*, 1988). The preliminary results from this expedition were presented in a paper by Francheteau *et al.* (1988). In another paper, Zukin and Francheteau (1990) have combined Seabeam data from the Rapanui expedition with five other expeditions (American and German) and have made a detailed assessment of the tectonics and plate boundaries in the areas depicted in Figure 1. In this paper we shall briefly show the results from our previous work, and then discuss how they have been used to test the location of the Pacific, Nazca, and Easter instantaneous Euler poles (Naar and Hey, 1989) and the kinematic microplate models recently devised by Engeln *et al.* (1988) and Schouten *et al.* (1988a and b).

MORPHOTECTONIC MAPS AND PLATE BOUNDARY CONFIGURATIONS

In order to make a detailed assessment of the tectonics along the northern and southern boundaries of the microplate, Zukin and Francheteau (1990) prepared a series of 200m contour interval bathymetric maps and a series of morphotectonic maps (Figs 2 and 3) which integrated these bathymetric data with other geological

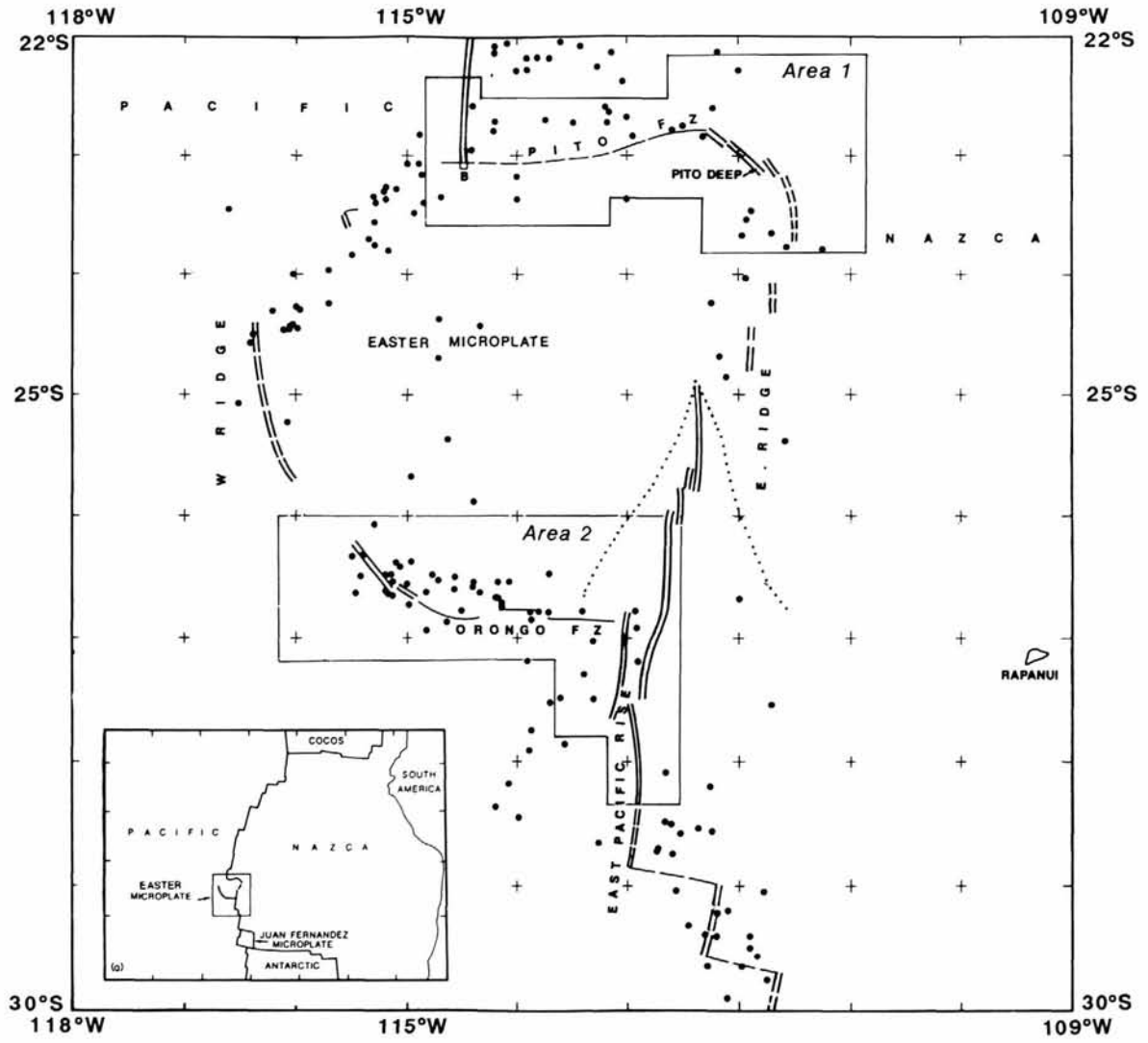

Figure 1

Location of the Easter Microplate in the SE Pacific (inset). Boundaries of the Easter microplate: Francheteau et al. *(1988), Naar and Hey (1986) and Hey* et al. *(1985). Double lines: spreading centre. Single line: transform fault. Dotted lines: pseudofaults of Hey* et al. *(1985). Dots: earthquake epicentres, from the World-Wide Standardized Seismographic Network (WWSSN). Boxes outline the two survey areas discussed in the text. Mercator projection.*
Position de la microplaque de l'île de Pâques dans le Sud-Est Pacifique (cartouche). Frontières de la microplaque : Francheteau *et al.* (1988), Naar et Hey (1986) et Hey *et al.* (1985). Traits doubles : zones d'accrétion. Trait simple : faille transformante. Lignes pointillées : pseudo-failles de Hey *et al.* (1985). Points : épicentres des séismes tirés de WWSSN. Les deux boites représentent les zones de cartographie détaillées discutées dans le texte. Projection de Mercator.

information: fault scarps (major and minor, taken from 20m-contour interval Seabeam charts); volcanic edifices; seismicity locations and published fault mechanisms; locations of dredges; relative motion vectors calculated from Naar and Hey's (1989) instantaneous Euler pole locations for the Pacific, Nazca and Easter plates. Using these data, and combining them with a preliminary investigation of the magnetic signature in these areas, Zukin and Francheteau (1990) made a detailed assessment of the northern and southern microplate boundary configurations, which differed significantly from the earlier configuration of Hey *et al.* (1985) (Fig. 4). There follows a brief discussion of the general findings of Francheteau *et al.* (1988) and Zukin and Francheteau (1990) along the northern and southern microplate boundaries.

THE NORTHERN BOUNDARY

The northern microplate boundary, delimited by area 1 (Fig. 1) is generally characterized, from east to west, by a ridge-transform intersection, a short E-W strike-slip zone, a transform zone under the influence of compressional deformation, and a RFF (ridge-fault-fault) Pacific-Nazca-Easter triple junction region (Fig. 4). The northeastern ridge-transform intersection is made up of a series of high relief horsts and graben, bounded by large, NW-SE en-echelon normal faults; the westernmost graben reaches the remarkable depth of 5 890m at 23°00'S, 112°56.5'W (the Pito Deep) and has been cited as the deepest rift axis mapped in the Pacific to date (Hey *et al.* 1985, Francheteau *et al.* 1988). The axis in this area

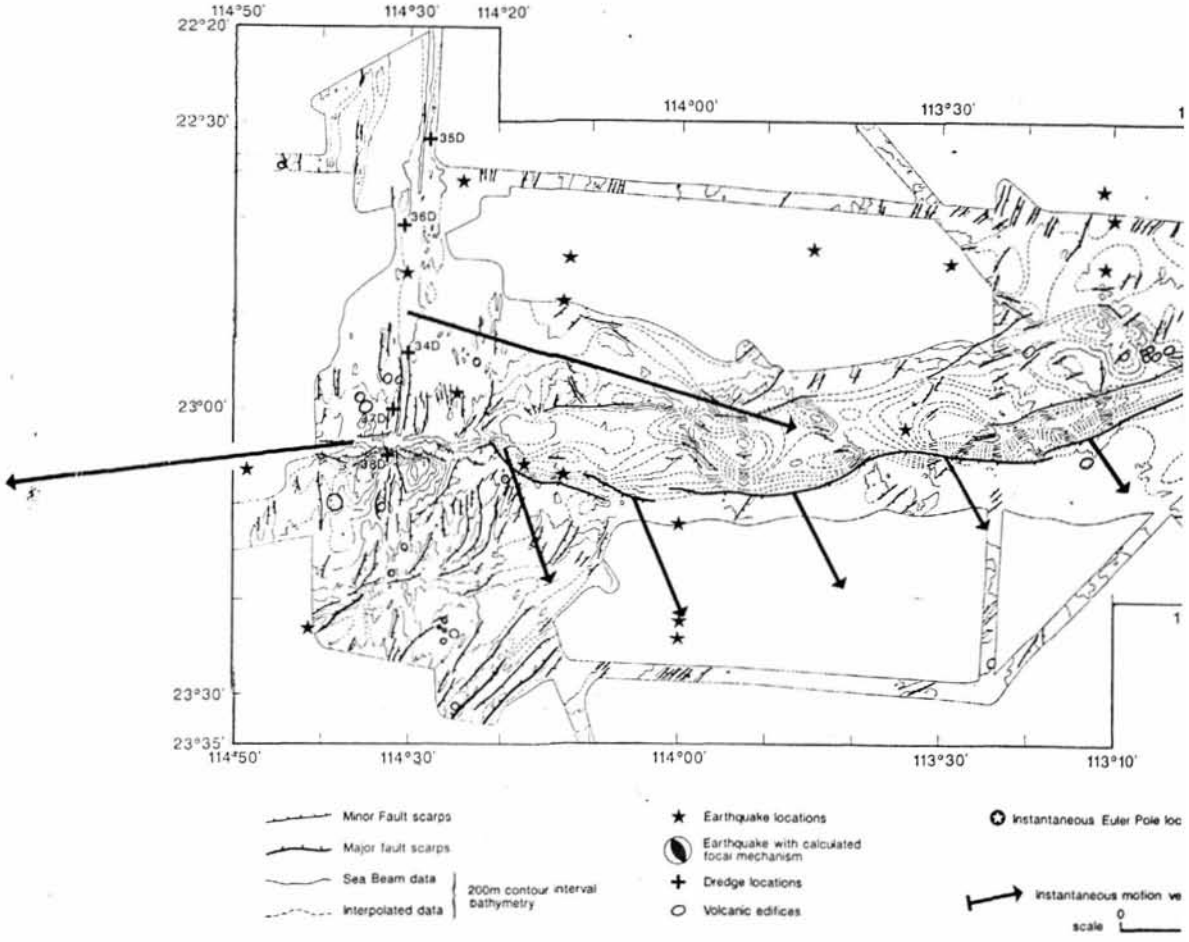

Figure 2

Morphotectonics of area 1. Northern microplate boundary, showing fault scarps (hatched lines; major scarps are depicted with thicker lines), volcanos (circles), seismicity (stars or fault mechanisms), dredges (crosses with number), location of the Nazca-Easter instantaneous Euler pole, calculated by Naar and Hey (1989), and relative motion vectors calculated from their instantaneous Euler Nazca-Easter, Pacific-Easter and Pacific-Nazca (first plate moving with respect to second plate) plate-pair-poles (Tab. 1). Mercator projection.

NORTHERN BOUNDARIES

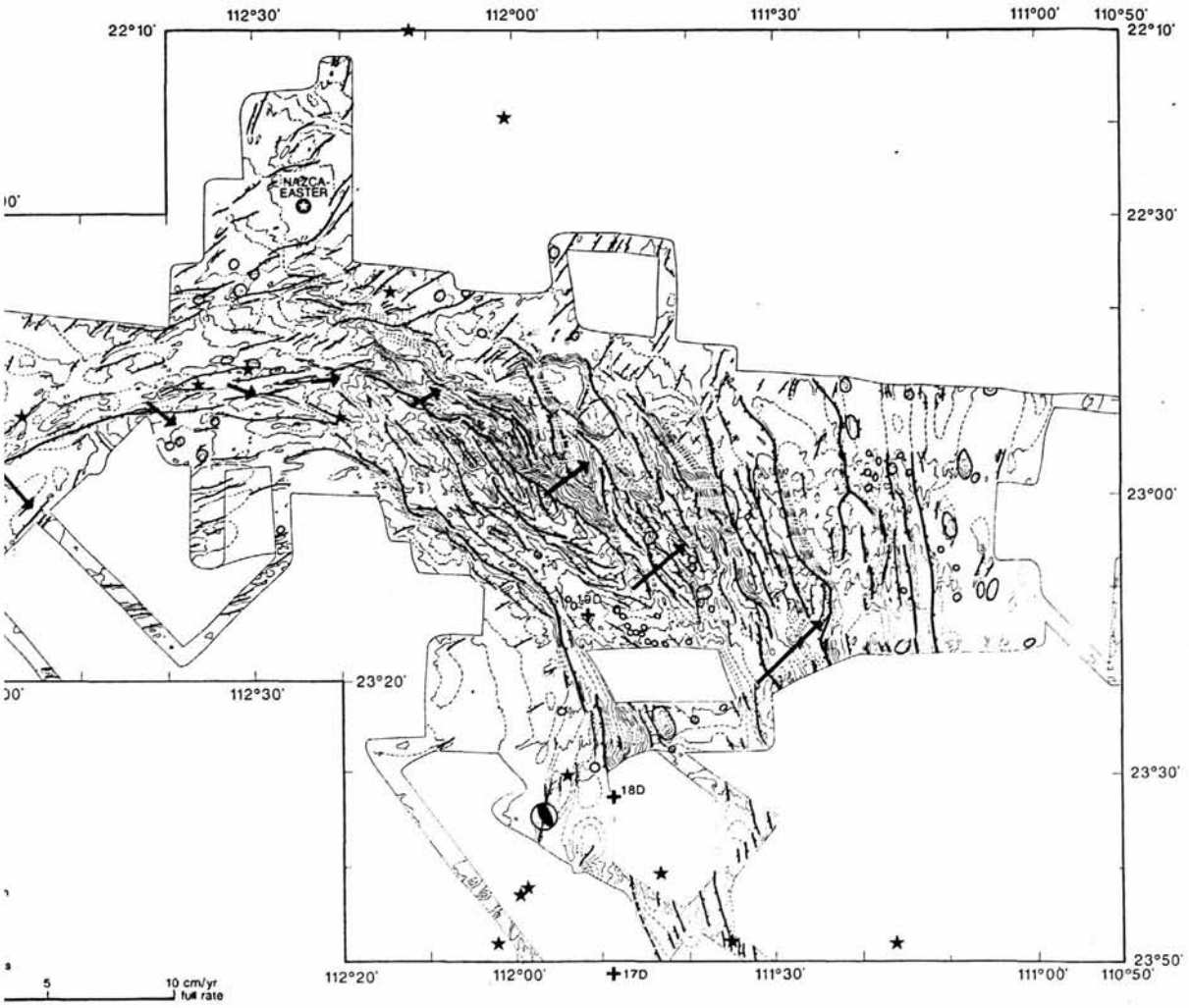

Carte morphotectonique de la zone 1. Frontière nord de la microplaque montrant les escarpements de faille (lignes avec barbules ; escarpements majeurs : lignes plus épaisses), volcans (cercles), séismes (étoiles ou mécanismes au foyer), dragages (croix avec numéro), position du pôle eulérien instantané Nazca-Pâques calculé par Naar et Hey (1989) et vecteurs - vitesse du mouvement relatif instantané Nazca-Pâques, Pacifique-Pâques et Pacifique-Nazca (le mouvement relatif est compté par rapport à la deuxième plaque citée) calculés à partir des pôles du tableau 1. Projection Mercator.

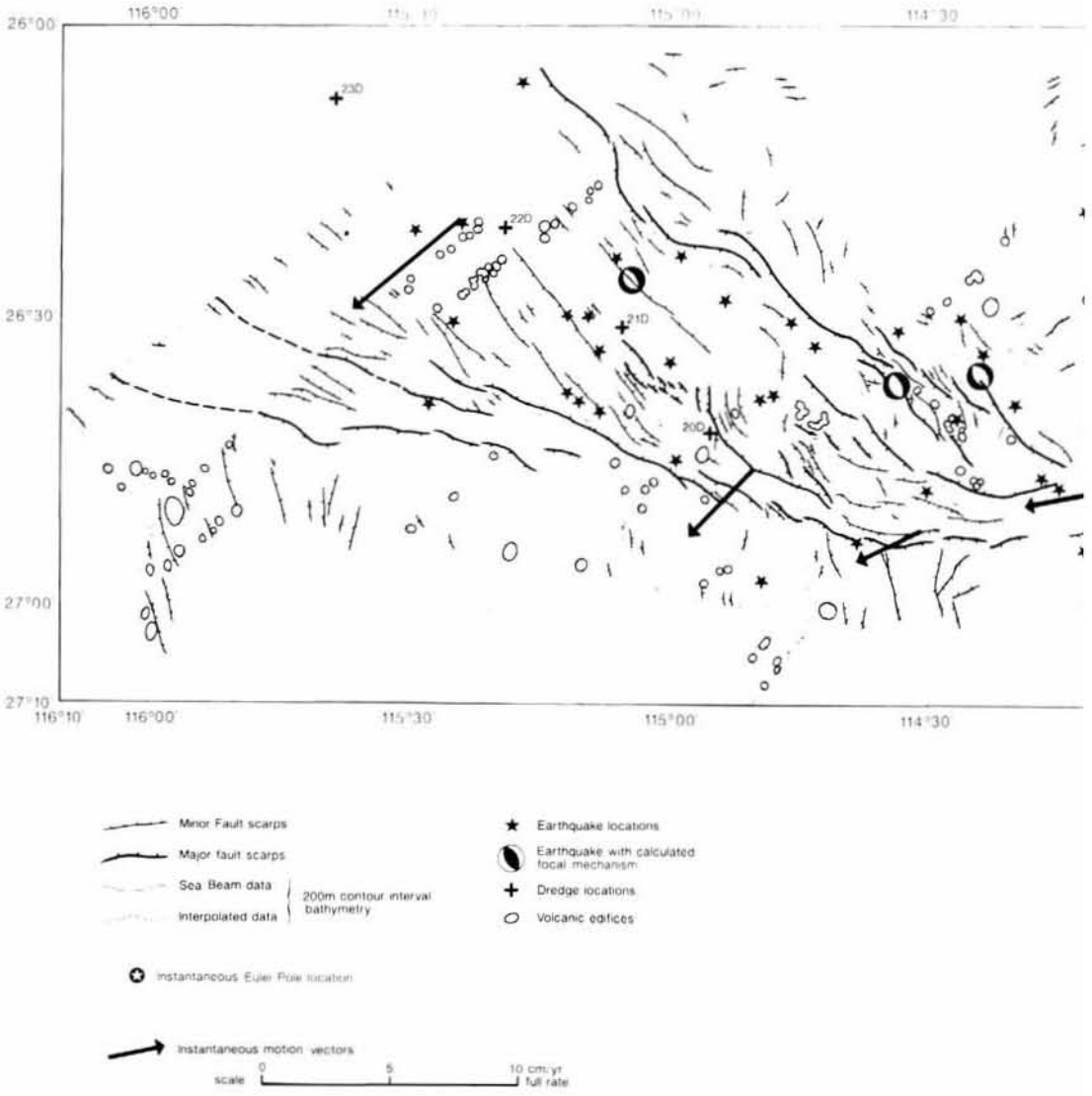

Figure 3

Morphotectonics of area 2. The southern microplate boundary: fault scarps (hatched lines, major scarps are depicted with thicker lines), volcanos (circles), seismicity (stars or fault mechanisms), dredges (crosses with number), location of the Pacific-Easter instantaneous Euler pole (Naar and Hey, 1989), and relative motion vectors calculated from their instantaneous Euler Nazca-Easter, Pacific-Easter, and Pacific-Nazca (first plate moving with respect to second plate) plate-pair-poles (Tab. 1). Mercator projection.

SOUTHERN BOUNDARY

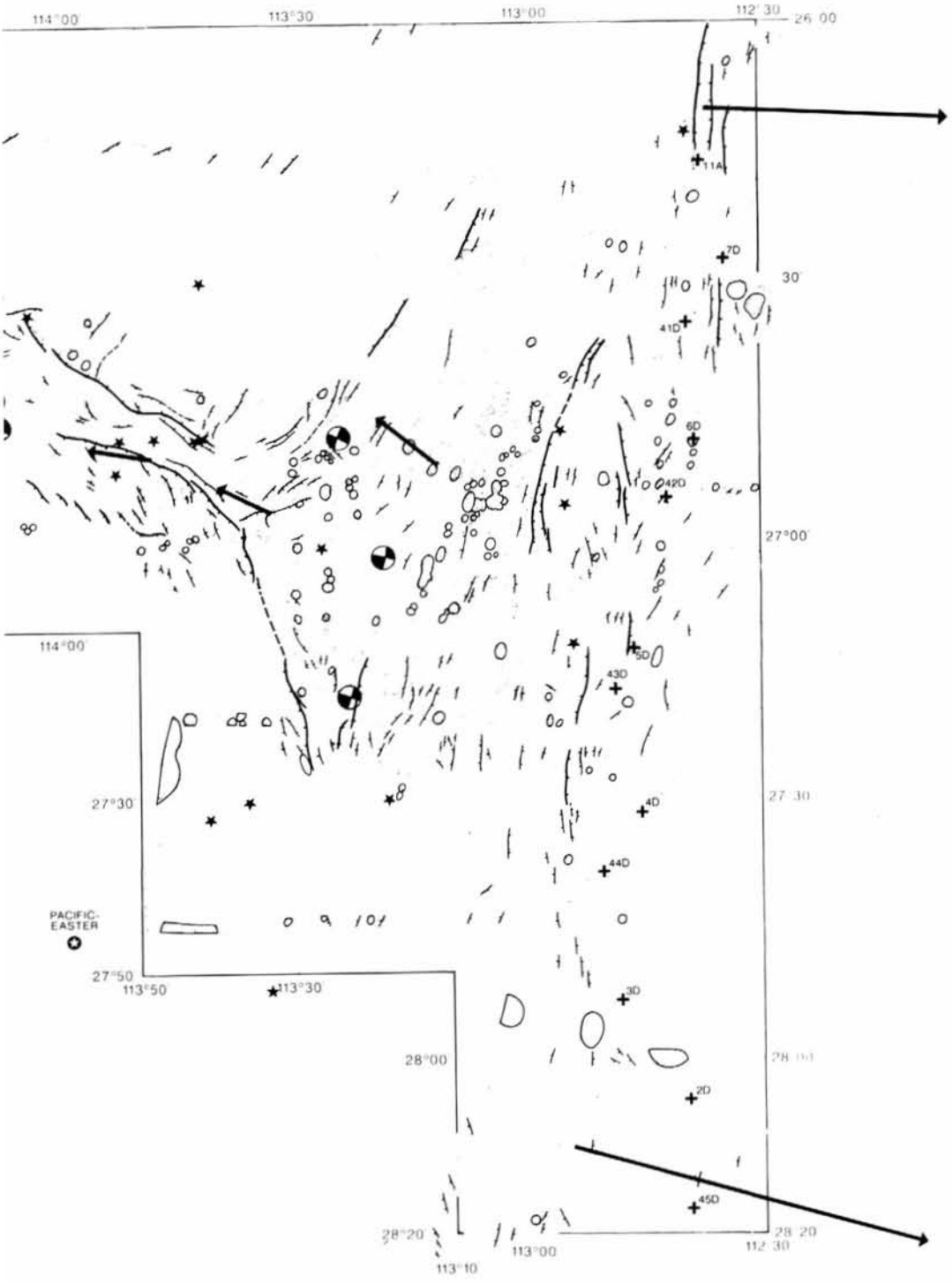

Carte morphotectonique de la zone 2. Frontière Sud de la microplaque : escarpements de faille (lignes avec barbules ; escarpements majeurs : lignes plus épaisses, volcans (cercles), séismes (étoiles ou mécanismes au foyer), dragages (croix avec numéro). Position du pôle eulérien instantané Nazca-Pâques (Naar et Hey, 1989) et vecteurs.- vitesse du mouvement relatif instantané Nazca-Pâques, Pacifique-Pâques et Pacifique-Nazca (le mouvement relatif est compté par rapport à la deuxième plaque citée) calculés à partir des pôles du tableau 1. Projection Mercator.

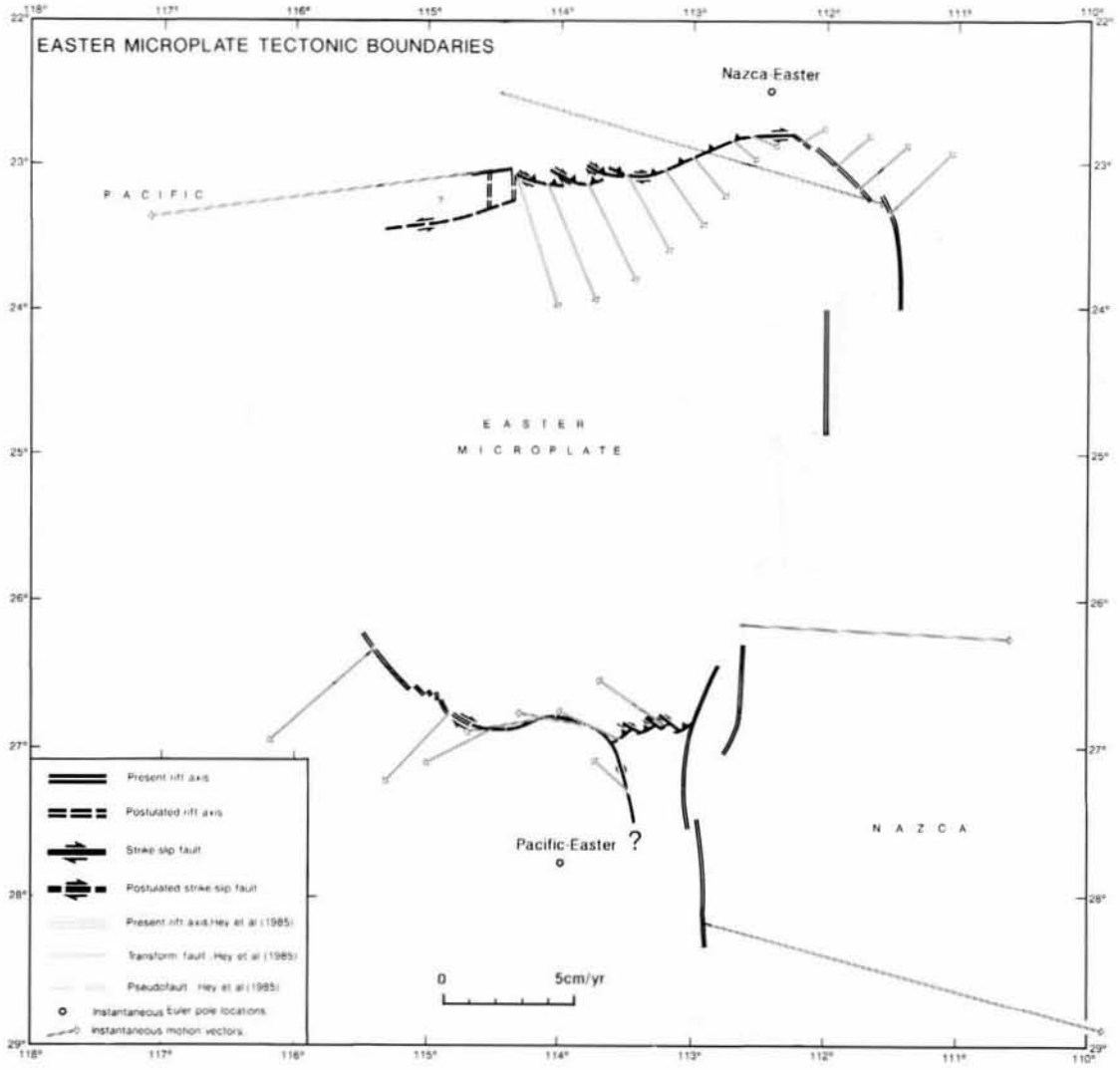

Figure 4

Comparison of tectonic boundaries of Hey et al. *(1985), in grey, and our new boundaries (Zukin and Francheteau, 1990), in black. Hey* et al. *(1985) boundaries: thick grey lines, spreading axis; thin grey lines, transform boundaries; dashed grey lines, pseudofaults. Zukin and Francheteau (1990) boundaries: double black lines, spreading axis; solid black lines, transform and/or compressional faults; dashed lines indicate possible abandoned or future rifting sites, or lack of constraint in boundary location. Also shown are locations of the Nazca-Easter and Pacific-Easter instantaneous Euler poles, calculated by Naar and Hey (1989), and relative motion vectors calculated from their instantaneous Euler Nazca-Easter, Pacific-Easter, and Pacific-Nazca (first plate moving with respect to second plate) plate-pair-poles (Tab. 1). Mercator projection.*
Comparaison entre les frontières de plaque de Hey *et al.* (1985), en gris, et celles de Zukin et Francheteau (1990), en noir. Frontières de Hey *et al.* (1985) : axes d'accrétion en lignes grises épaisses, failles transformantes en lignes grises fines, pseudo-failles en lignes grises pointillées. Frontières de Zukin et Francheteau (1990) : axes d'accrétion en lignes noires doubles, failles transformantes et/ou zones de compression en lignes noires continues les lignes pointillées indiquent les zones d'accrétion fossiles (ou futures) ou les zones frontières mal déterminées. On a aussi marqué la position des pôles euleriens instantanés pour les mouvements Nazca-Pâques et Pacifique-Pâques déterminés par Naar et Hey (1989) et les vecteurs-vitesse du mouvement relatif instantané Nazca-Pâques, Pacifique-Pâques et Pacifique-Nazca (le mouvement relatif est compté par rapport à la deuxième plaque citée) calculés à partir des pôles du Tableau 1. Projection Mercator.

is made up of a series of left lateral offsets and the morphology here may be indicative of either discontinuous northwesterly ridge propagation (the horsts to the N and E of the Pito Deep representing the propagating rift pseudofaults) or northwesterly ridge jumping. The northernmost rift axis leads westward to a short, low relief, purely E-W right-lateral strike-slip zone, between 112°20'W and 112°47'W, which marks the beginning of the Pito Transform Zone. West of 112°47'W, this transform zone turns to the SW and is present as an elongated ridge which increases in height westward. Between 113°20'W and 114°20'W, the transform zone turns to 275°, and is present as a series of NW-SE orientated en-echelon ridges. This entire ridge system is thought to be controlled by translational as well as compressional motion; the compressional motion augments and turns to a more N-S direction toward the west, as indicated by the increase in relief and the change in trend of this relief, to the west. This transform zone is interpreted as being bounded by thrust faults to the south and by right-lateral strike-slip faults on the SW side of the en-echelon highs (Fig. 4). West of the Pito Transform Zone, at 23°02.5'S, 114°31.5'W, lies the RFF Pacific-Nazca-Easter triple junction. A fracture zone or fault zone, trending 225° lies south of this RFF triple junction, near 23°18'S, which separates N-S structures to the north

from NE-SW structures to the south. A rapid morphologic and tectonic change is observed across the Pito Transform zone at 114°20'W. Several new boundary configurations for this triple junction region have been suggested by Zukin and Francheteau (1990), including (Fig. 4):

- a small NW microplate block, bordered to the south by a left lateral transform fault, and to the east and west by rifts, implying a second RFF triple junction near 23°05'S, 114°20. 25'W;
- extension of the EPR to the south in the past;
- an old fracture zone existing to the south of the present triple junction.

THE SOUTHERN BOUNDARY

The southern microplate boundary, delimited by area 2 (Fig. 1) is generally characterized, from west to east, by a series of left-laterally offset spreading centres, a right-laterally slipping, tectonically complex, transform zone, and an overlapping spreading centre (OSC) (Fig. 4). In detail, to the west we observe a large, "V-shaped" (in plan view) ridge system, with an eastward pointing tip near 26°45'S, 114°10'W, which separates younger oceanic crust between the ridges from older oceanic crust to the north and south of the ridges. The valley floor between the two "V-shaped" ridges is characterized by a series of left-laterally offset graben (bounded by NW-SE en-échelon normal faults), some of which have been interpreted as active rifting sites. The "V-shaped" ridges may be indicative of a southward propagating western rift (they may represent the pseudofaults of this propagating rift). The easternmost rifting site, at 26°46'S, 114°50'W, gives way to a right lateral transform fault which runs along the southern side of the southernmost ridge, located near 26°50'S, 114°35'W. Shear structures observed to the NE of the easternmost rifting site, near 26°35'S, 114°55'W, may possibly be indicative of a developing transform boundary or overlap region, and a developing rifting site to the NE of the currently active rift, near 26°30'S, 114°45'W. At 26°45'S, 114°10'W, the "V-shaped" ridges coalesce into a single, complex ridge system, which curves dramatically to the SSE, loses height quickly eastward, and is thought to be dominated by right-lateral strike-slip motion. East of this ridge system (east of 113°25'W), the southern Pacific-Nazca-Easter triple junction region is generally characterized by low relief, and consists, to the west, between 113°00'W and 113°30'W, of a series of ridges and depressions and, to the east, centred near 26°50'S, 112°50'W, of a large, N-S trending, overlapping spreading centre (OSC). Three possible boundary configurations for this triple junction region have been proposed by Zukin and Francheteau (1990)(Fig. 4):

- a RRF triple junction, located at 26°50'S, 113°00'W, at the intersection of the western OSC branch to the east and a tectonically complex, right-laterally slipping transform boundary, containing compressive as well as strike-slip fault boundaries, to the west;
- a right lateral transform boundary extending south along the large SSE curving ridge, near 26°55'S, 113°35'W, and consequently an unidentified triple junction, located somewhere south of 27°25'S;
- a wide zone or "wedge" of deformation, between the Pacific, Nazca, and Easter plates, centred near 27°05'S, 113°15'W.

TEST OF PACIFIC-EASTER AND NAZCA-EASTER INSTANTANEOUS EULER POLE LOCATIONS

On the basis of our detailed tectonic and geophysical information along the northern and southern microplate boundaries, we can use two methods to make a test of the most recently calculated instantaneous Euler pole locations for the Pacific-Easter and Nazca-Easter plate pairs (Naar and Hey, 1989). The first, and more qualitative, test is to compare, at various locations, the deformational regimes (extension, strike-slip motion, or compression) predicted by the Euler pole locations (and locations of the limits between these regimes) with the deformational regimes interpreted on the basis of our new plate boundary configurations. The second and more quantitative test, is to test accretion rates by making precise comparisons between our magnetic data profiles and magnetic models which have been calculated (using Naar and Hey's (1989) instantaneous Euler pole locations) at the specific point where these profiles cross the spreading rift axis.

Naar and Hey (1989) calculated instantaneous Euler pole locations for the Pacific, Nazca, and Easter plates, using two different inversion methods. One set of poles is calculated using three plates and requires closure for the three rotation vectors; the other is calculated using only data involving the two plates concerned. These authors found that the two sets of pole locations were very similar, suggesting that the microplate is behaving in an essentially rigid manner. In this study we test the validity of the three-plate-closure pole locations.

The Nazca-Easter instantaneous Euler pole was determined by Naar and Hey (1989) using spreading rates estimated from seven magnetic profiles across the Easter microplate eastern rift, at latitudes between 26°48'S and 25°00'S. The Pacific-Easter Euler pole was computed using six magnetic profiles along the Easter microplate western rift, at latitudes between 23°48'S and 26°24'S, and one magnetic profile which crosses the axis at 22°36'S, 114°29'W. Their calculation also included four transform azimuths, located along the northern part of the western rift, which were obtained from Seamarc II data (Hey and Naar, 1987), and four slip vectors along the SW rift, derived from earthquake first motions (Engeln and Stein, 1984). The Nazca-Pacific

Table 1

Location of Naar and Hey's (1989) instantaneous Euler Nazca-Pacific, Nazca-Easter, and Pacific-Easter plate-pair-pole locations, angular rotation of plate-pair-poles (degrees/Ma), and vectors calculated from these poles (centimetres/a, direction of first plate moving with respect to second plate, in degrees from north). Chosen plate boundary points are indicated numerically, points along magnetic profiles, utilized in magnetic modelling, are indicated with an "M". The pole positions follow the convention of Le Pichon et al., *1973.*
Position des pôles Eulériens instantanés, Nazca-Pacifique, Nazca-Pâques et Pacifique-Pâques (rotations angulaires en degrés/Ma). Vecteurs - vitesse calculés à partir de ces pôles (module en cm/an, direction en degrés par rapport au Nord. Les points courants sur les frontières sont numérotés, les points sur les profils magnétiques utilisés sont annotés avec la lettre M. La position des pôles suit la convention de Le Pichon *et al.* (1973).

	Data		Latitude	Longitude	Angular Rotation (deg/ma) or Relative Motion Rate (cm/a)	Relative Motion Direction
Nazca-Pacific	Pole:		46.77	-91.76	1.463	
	Vectors:	1	-22.50	-114.47	15.5	106
		2	-22.83	-114.50	15.5	106
		3	-27.33	-113.05	15.8	105
		4	-28.17	-112.91	15.9	105
Nazca-Easter	Pole:		-22.49	-112.41	14.99	
	Vectors:	1	-23.33	-111.5	33.4	46
		2 (M109)	-23.17	-111.78	2.6	49
		3	-23.00	-111.9	41.9	49
		4	-22.83	-112.20	1.1	60
		5	-22.80	-112.39	0.9	82
		6	-22.80	-112.55	1.0	114
		7	-22.83	-112.72	1.3	130
		8	-22.95	-113.00	2.11	40
		9	-23.04	-113.22	2.7	144
		10	-23.07	-113.50	3.4	150
		11	-23.14	-113.79	4.2	153
		12	-23.14	-114.08	4.9	157
		13	-23.07	-114.33	5.4	162
		14	-26.17	-112.61	10.7	93
		M114	-23.14	-111.82	2.5	50
		M116	-23.10	-111.84	2.3	49
		M118	-23.07	-111.86	2.2	49
Pacific-Easter	Pole:		-27.77	-113.98	14.60	
	Vectors:	1	-23.05	-114.61	13.42	63
		2	-26.33	-115.40	5.4	229
		3	-26.76	-114.83	3.6	223
		4	-26.86	-114.50	2.9	243
		5	-26.67	-114.33	3.2	254
		6	-26.79	-114.17	2.8	260
		7	-26.83	-113.80	2.7	280
		8	-26.94	-113.55	2.6	295
		9	-27.28	-113.50	1.8	311
		10	-26.83	-113.27	3.2	304
		M26	-26.35	-115.38	5.4	229
		M30	-26.41	-115.32	5.1	229
		M32	-26.55	-115.21	4.6	228

instantaneous Euler pole was calculated using twenty-five magnetic profiles, six transform azimuths and sixteen earthquake slip vectors, along the EPR, at latitudes between 3°42'S and 31°24'S.

To qualitatively test the instantaneous Euler pole locations, we have calculated relative motion vectors for the three plate pairs at points along our new plate boundaries. These vectors (relative motion rate and relative motion direction), and their locations, are given in Table 1, and are shown plotted in both the morphotectonic maps (Figs 2 and 3) and in the microplate boundary configuration map (Fig. 4). It may be seen that, along the northern microplate boundary, the Nazca-Easter instantaneous Euler pole implies extension east of 112°20'W, a change to strike-slip motion at this location, a short (approximately 20 km long), pure E-W strike-slip zone (from 112°20'W to 112°30'W), and further to the west, increasing compressional motion which trends closer to N-S towards the west. Along the southern microplate boundary, the Nazca-Easter Euler pole location predicts extension across the Nazca-Easter ridge axis and across the northern branch of the OSC. These observations indicate that the Naar and Hey (1989) Nazca-Easter instantaneous Euler pole location is in good agreement with our data.

Along the southern microplate boundary, the Pacific-Easter Euler pole location implies extension across the SW rift axis, turning to pure right-lateral strike-slip motion near 114°20'W. Across the proposed future rifting site, located to the NE of the current rift axis,

extensional elements are predicted eastward up to 114°10'W. East of 114°20'W, the pole implies principally strike-slip deformation along our plate boundary as far as 113°35'W, east of which the plate boundary location is poorly constrained. Along our E-W mixed compressional and right-lateral strike-slip transform boundary, the Pacific-Easter Euler pole implies compression to the SE and NW-SE orientated right-lateral strike-slip boundaries. Along the NNW-SSE trending right-lateral transform boundary, located approximately along 113°30'W, rotation about the Pacific-Easter Euler pole would lead to NW-SE orientated right-lateral slip. Looking at the northern microplate boundary, the Pacific-Easter Euler pole implies E-W left-lateral strike-slip motion across the hypothesized left-lateral transform fault found west of the RFF Pacific-Nazca-Easter northern triple junction. All of these predictions appear to agree well with our boundary configurations along the southern and northern microplate boundaries, lending support to the Naar and Hey (1989) Pacific-Easter instantaneous Euler pole location.

To make our more quantitative magnetic modelling test, we first turn to the magnetic anomalies collected over the Pito Deep area (Fig.5a). As a first step, we have made identifications of the magnetic anomalies in the area by comparing the data profiles with a standard theoretical profile, calculated using the Naar and Hey (1989) Nazca-Easter instantaneous Euler pole. Each of these profiles has been projected to a theoretical spreading direction, calculated for the point of intersection of each magnetic profile with the supposed rift graben centre. A similar process was followed (using the Nazca-Pacific instantaneous Euler pole of Naar and Hey, 1989) for identification of magnetic anomalies to the north of the rift graben in this area, in order to obtain a clear distinction between the anomalies in the south, created by the Pito rift, and those to the north, created by the EPR. Details of these identifications can be found in Zukin and Francheteau (1990), and the results are illustrated in Figure 5a. We see that the central anomaly has been clearly identified in the southern Pito Deep area, and the possible identification of anomalies 2 and 2a to the east and anomaly 2 to the west of the central anomaly. To the north and east, anomalies 2a and part of anomaly 3, created on the East Pacific Rise to the north of the Easter microplate, have been identified. The change in trend between these anomalies attest to the validity of our interpretation that they originated at different rifting sites.

Since our aim is to test the Naar and Hey (1989) instantaneous Nazca-Easter Euler pole, we shall now compare the precise form of the central anomaly identified on several of the southernmost of these data profiles, with the form of a modelled central anomaly. Four of the profiles (M109, M114, M116, M118), projected to the calculated spreading direction (Tab. 1), are illustrated in Figure 5b, along with two model profiles, one calculated for profile M109 and the other for profile M118. We see that the form and width of the central anomaly in data profile M109 agrees well with the calculated model. The location of anomaly 2 is not the same for the observed profile and the model, but we consider this of little importance to our test, since we are testing an *instantaneous* pole. This observation may indicate that the spreading rate here increased rapidly between 2 ma and 0.7 ma. In comparing the data profile M118 to the model profile, we see that the form of the central anomaly is less clear here than further to the south. If our chosen Brunhes/Matuyama boundary locations (as depicted in Fig. 5b) are correct, the width of the central anomaly is considerably greater in the data profile than in the model profile. This indicates a greater instantaneous spreading rate here than predicted by the Naar and Hey (1989) Nazca-Easter instantaneous Euler pole. The locations of anomalies 2 and 2a agree well with the model profile. These observations along data profile M118 indicate, as in profile M109, that there has been a rapid increase in spreading rate between 2 ma and 0.7 ma. The observation that the central block widens to the the north in the data profiles and narrows to the north in the model profiles is puzzling, as it may suggest that the Nazca-Easter instantaneous Euler pole lies to the south of the Pito Deep area, rather than to the north. It must however be taken into account, when discussing changes in spreading rate and/or pole position, that the magnetic signature in this area could well have been disrupted by tectonic complications such as ridge propagation, ridge jumping and/or asymmetric spreading.

We turn now to the magnetic anomalies collected over the SW rift, in order to test Naar and Hey's (1989) Pacific-Easter instantaneous Euler pole location for this region (Fig. 6a). Zukin and Francheteau (1990) modelled data as for the Pito Deep area in order to identify magnetic anomalies there (Fig. 6a). To the west, the central anomaly has been clearly identified on the first three profiles. The Brunhes/Matuyama boundary is observed to extend eastward on the south side of the central anomaly, to profile M48, and is characterized by several left-lateral offsets. The three profiles on which the central anomaly has been observed (M26, M30 and M32) have been projected to the theoretical spreading direction (calculated for the point on that profile which traverses the spreading axis, Tab. 1), and are depicted in Figure 6b. Two model profiles are shown in figure 6b, one calculated for profile M26 and the other for profile M32. We see that the form and width of the central anomaly for all three profiles generally agree well with the modeled anomalies, but in detail, the central anomaly of data profile M26 appears to be slightly narrower in the model. These observations may indicate that the instantaneous Pacific-Easter Euler pole of Naar and Hey (1989) could be located slightly further to the east.

The results of our qualitative and quantitative tests of the Naar and Hey (1989) instantaneous Euler pole locations for the Nazca-Easter and Pacific-Easter plate pairs indicate that these pole locations are, in a general sense, acceptable. They accurately predict our new plate

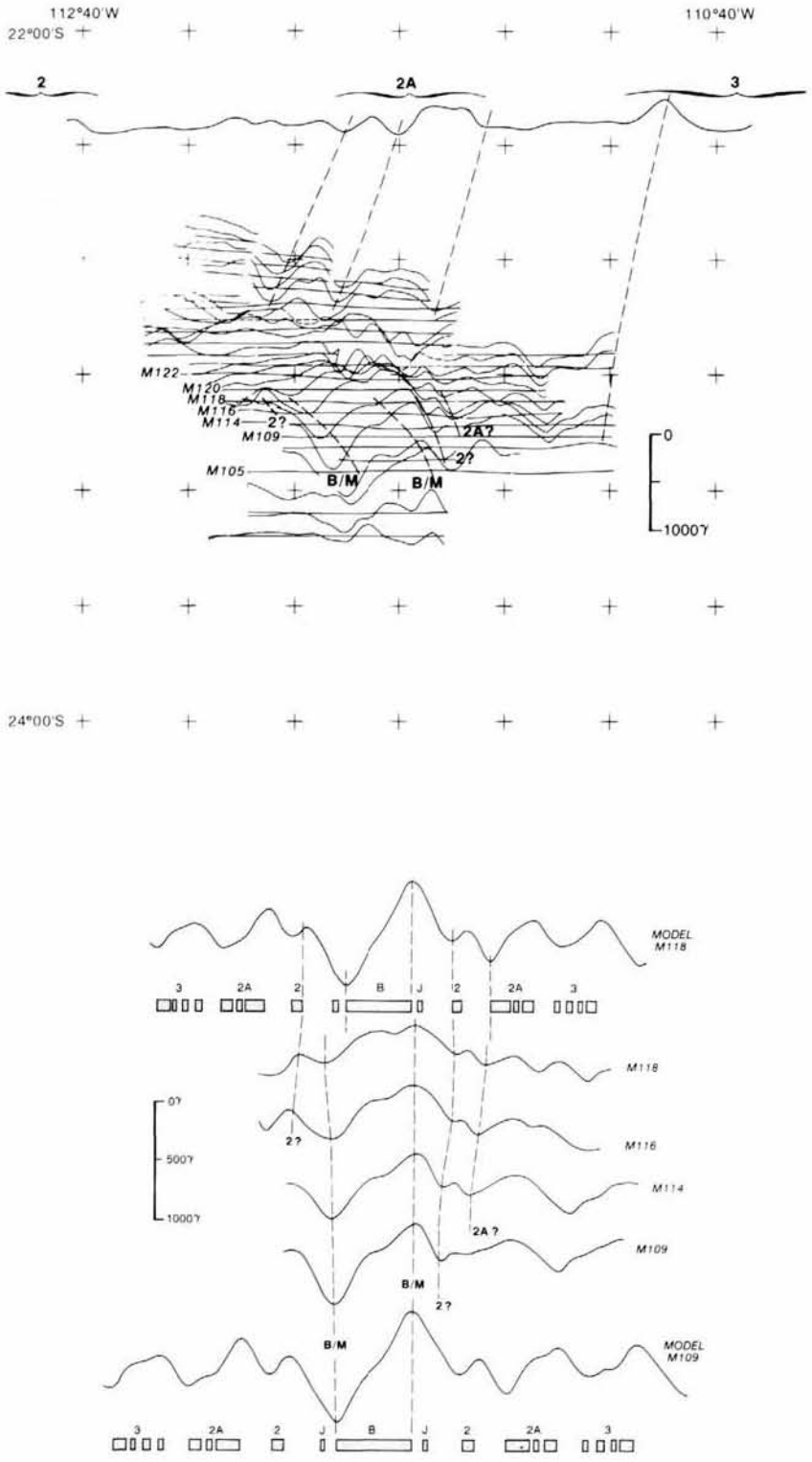

Figure 5

a. *Magnetic profiles for the Pito Deep area, in geographic frame, profiles projected north. Dashed lines : magnetic anomaly identifications of Zukin and Francheteau (1990). Locations of magnetic profiles used in modelling are indicated. Mercator projection.*
b. *Magnetic data profiles M109, M114, M116, M118, projected to spreading direction, as calculated from the point where the magnetic profile crosses the spreading rift axis, and utilizing the Nazca-Easter instantaneous Euler pole of Naar and Hey (1989). Also shown are magnetic models calculated for profiles M109 and M118, using: computed spreading rate and direction (Tab. 1); depth model of Parsons and Sclater (1977), with ridge axis at 3 km depth; assumed symmetry in spreading; contamination factor of 0.7 (Tisseau and Patriat, 1981). Dashed lines represent magnetic anomaly markers of the model profiles and identifications along the data profiles (Zukin and Francheteau, 1990).*

a. Profils magnétiques de la région du fossé de Pito. Les profils sont projetés vers le Nord. Les lignes pointillées montrent les identifications d'anomalies magnétiques de Zukin et Francheteau (1990). Les profils utilisés pour la comparaison avec les modèles sont annotés. Projection Mercator.
b. Profils magnétiques M109, M114, M116 et M118 projetés dans la direction d'ouverture Nazca-Pâques calculée au point où chaque profil coupe l'axe du rift d'après le pôle eulérien instantané Nazca-Pâques de Naar et Hey (1989). On montre 2 modèles magnétiques pour la position des profils M109 et M118 calculés avec les paramètres suivants : taux et direction d'ouverture d'après le Tableau 1, profondeur d'après le modèle de Parsons et Sclater (1977) avec une profondeur à l'axe de 3 km, accrétion symétrique, facteur de contamination 0,7 (voir Tisseau et Patriat, 1981). Les lignes pointillées corrèlent les anomalies des modèles et des profils observés (Zukin et Francheteau, 1990).

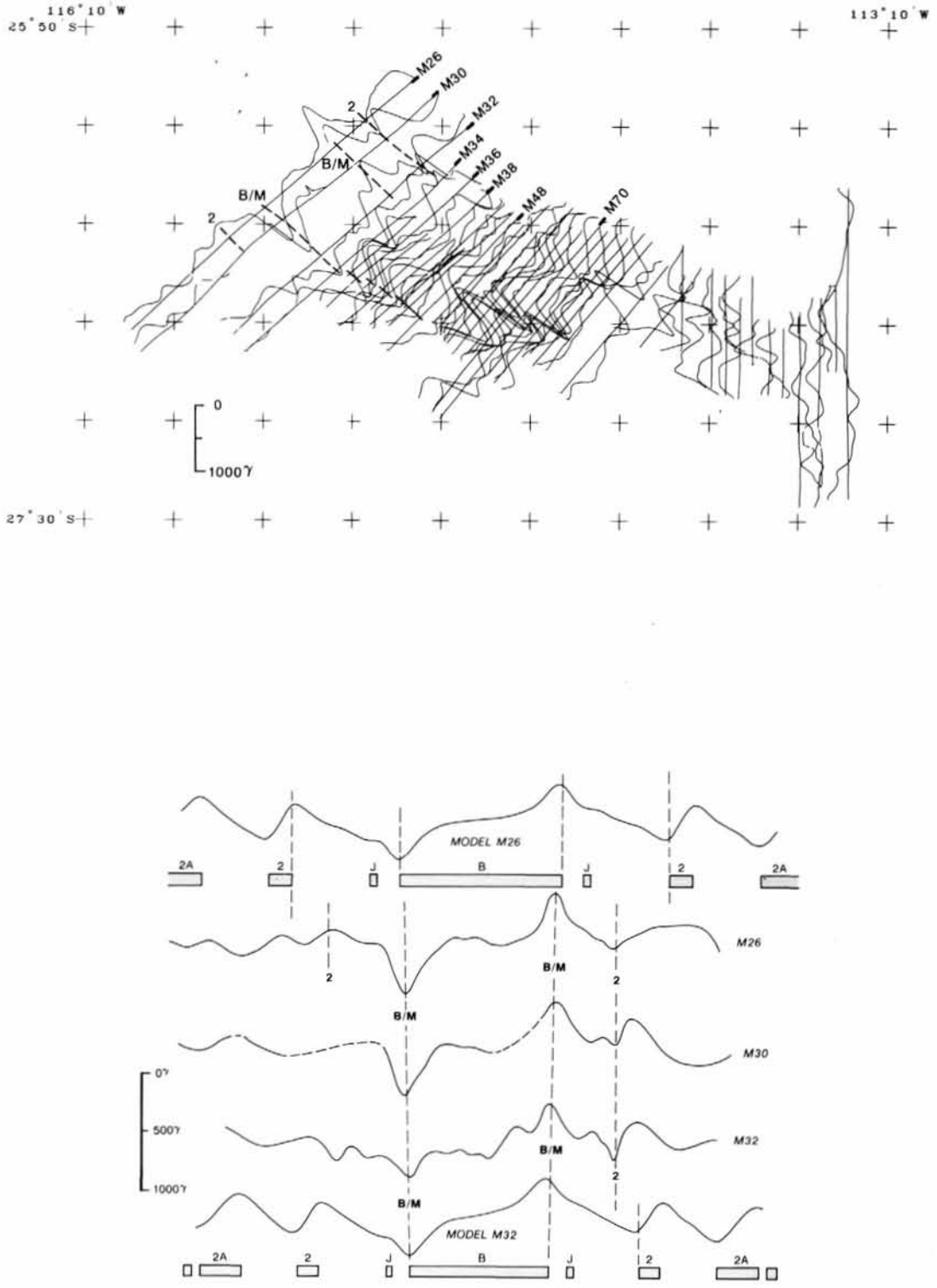

Figure 6

a. *Magnetic profiles for the SW rift area, in geographic frame, profiles projected west. Dashed lines: magnetic anomaly identifications of Zukin and Francheteau (1990). Locations of magnetic profiles are indicated. Mercator projection.*
b. *Magnetic data profiles M26, M30, M32 projected to spreading direction, as calculated from the point where the magnetic profile crosses the spreading rift axis, and utilizing the Pacific-Easter instantaneous Euler pole of Naar and Hey (1989). Magnetic models : points along profiles M26 and M32, using: computed spreading rate and direction (Tab. 1); depth model of Parsons and Sclater (1977), with ridge axis at 3 km. depth; assumed symmetry in spreading; contamination factor of 0.7 (Tisseau and Patriat, 1981). Dashed lines represent magnetic anomaly markers of the model profiles and identifications along the data profiles (Zukin and Francheteau, 1990).*
a. Profils magnétiques de la région Sud-Ouest. Les profils sont projetés vers l'Ouest. Les lignes pointillées : identifications d'anomalies magnétiques de Zukin et Francheteau (1990). Les profils utilisés pour la comparaison avec les modèles sont annotés. Projection Mercator.
b. Profils magnétiques M26,M30,M32 projetés dans la direction d'ouverture Pacifique-Pâques calculée au point où chaque profil coupe l'axe du rift d'après le pôle eulérien instantané Pacifique-Pâques de Naar et Hey (1989). 2 modèles magnétiques : position des profils M26 et M32 calculés pour les paramètres suivants : taux et direction d'ouverture d'après le Tableau 1, profondeur d'après le modèle de Parsons et Sclater (1977) avec une profondeur à l'axe de 3 km, accrétion symmétrique, facteur de contamination 0.7 (Tisseau et Patriat, 1981). Les lignes pointillées concèdent les anomalies des modèles et des profils observés (Zukin et Francheteau, 1990).

boundary configurations and the general form of the central anomaly. Some disagreements arise when the magnetic data and magnetic models are compared in a precise manner, especially for the Nazca-Easter plate-pair Euler pole. This may be due to the lack of magnetic data north of 25°00'S, utilized in Naar and Hey's (1989) inversion for the Nazca-Easter pole, indicating the need to collect additional data along the microplate boundaries. Alternatively, problems in the magnetic modelling may arise due to tectonic complications in the areas studied, as discussed previously for the Pito Deep area. We therefore tend to give more weight to our more qualitative testing methods.

DISCUSSION OF MICROPLATE MODELS

We turn now to a discussion of our observations with reference to the recently proposed kinematic microplate models of Engeln *et al.* (1988) and Schouten *et al.* (1988a and b). Engeln *et al.* (1988) introduced two kinematic microplate models, one for rigid behaviour, and the other for a zone of simple shear. Their rigid microplate model suggests that the microplate is bordered to the east by a propagating, growing ridge, and to the west by a propagating, dying ridge. The microplate Euler poles lie close to the northern and southern boundaries. As a result of this geometry, the microplate rotates clockwise in time, and the southern transform boundary evolves into a slow, obliquely spreading centre. In this model, the relative motion across the southern, dying ridge changes direction in time. Engeln *et al.* (1988) suggest that this change could be accommodated in several ways:

- transforms may reorient in order to remain parallel to the relative motion;
- or ridges may propagate and die to maintain a continuous boundary, while spreading obliquely.

These authors also suggest that ridge segments may reorient to allow orthogonal spreading, or that transform boundaries may acquire extensional or compressional components of motion, and suggest that this reorganization may disrupt the tectonic and magnetic signatures of the SW spreading region. This model predicts that when the southernmost point on the western ridge ceases to spread, the southern boundary will begin to migrate northwards. It also suggests that the northern boundary is dominated by compressional deformation. In the simple shear model, the response to differential spreading between the growing and dying ridges is taken up by pervasive simple shear, which is parallel to the spreading direction, as opposed to rigid rotation of the microplate.

The geometry of the two models is similar, but the predicted evolution of the northern and southern boundaries shows large differences. In the case of the shear model, both of these boundaries remain transforms; motion across the initial southern transform zone decreases with time, while that on the northern boundary increases with time, until it becomes a transform between the two large plates, and the shear zone vanishes. In the case of rigid rotation, the boundaries are characterized by complex and rapidly evolving deformational structures; in general, the northern boundary primarily contains components of compressional deformation, while the southern boundary is characterized by oblique extension.

Our observations support the rigid plate model and oppose the shear model of Engeln *et al.* (1988). Evidence that the northern and southern boundaries of the microplate are not simple, strike-slip transform zones refutes arguments for the shear model. In support of the rigid plate model, we see compressional deformation along the northern boundary, and we are in general agreement with the Nazca-Easter and Pacific-Easter plate-pair instantaneous Euler pole locations of Naar and Hey (1989), which lie close to the microplate boundaries. The NE-SW fabric observed on the microplate interior (Hey *et al.*, 1985; Searle *et al.*, 1989) may also be indicative of rigid rotation of the microplate (first suggested by Hey *et al.*, 1985). Although we see no strong tectonic evidence for oblique spreading, reorientation of transforms, or propagating rift segments along the SW rift, we suggest that oblique motion along this rift is taken up by reorientation of ridge segments, as is evidenced by a disrupted magnetic signature and frequent, contemporary ridge offsets (or overlaps) which often differ in offset length from their respective Brunhes/Matuyama offsets (Zukin and Francheteau, 1990). We also have made observations which agree with the idea of Engeln *et al.* (1988) that, in a rigid rotation model, transform motion along this boundary may acquire compressional and/or extensional elements. It is important to note that although our contemporary observations support the rigid plate model of Engeln *et al.* (1988), this does not indicate that the microplate has always behaved as such; it may have been dominated by shear behaviour in the past.

The kinematic microplate model proposed by Schouten *et al.* (1988a and b) assumes rigid behaviour and suggests that microplate motion can be described by steady velocity of a point and rotation about that point (second order motion), so that the geometry of the microplate system resembles that of a ball bearing. This model is similar to the rigid plate model of Engeln *et al.*, (1988). Schouten *et al.* (1988a and b) propose that the microplate Euler poles lie precisely on the microplate boundaries, at the tip of the northern and southern propagating ridges. The Euler pole locations are the unique points where there is no relative movement of the microplate with respect to the larger oceanic plates, and are also the points where extension changes to compression along the microplate boundary. These Euler pole locations move with a velocity equivalent to that at which the microplate rotates about a microplate rotation pole located near its center, thus implying propagation of the eastern and western rifts, leaving characteristic "pseudofault" traces.

We find that there is quite close, but not rigorous agreement, between the model of Schouten *et al.* (1988a and b) and our tectonic interpretation. As an example, we believe that the microplate Euler rotation poles do not lie precisely on the microplate boundaries. Our observations support the Nazca-Easter and Pacific-Easter instantaneous Euler pole locations of Naar and Hey (1989), which lie approximately 75 km south, and 25 km north of the plate boundaries, respectively. If, as Schouten *et al.* (1988a and b) predict, the NE and SW rifts are propagating rifts and the horsts in the Pito Deep area, as well as the high "V" shaped ridges in the SW rift area, represent "pseudofaults", we note that their configurations (especially in the Pito Deep area) do not match well with the "pseudofault" configuration shown in their model. Although the Schouten *et al.* (1988a and b) model does not hold in a rigorous fashion to our observations, it does help to explain the general geometry and tectonic character of the microplate, and in this sense, it, together with the Engeln *et al.* (1988) rigid plate model, are important steps in helping us to understand microplate kinematics.

CONCLUSIONS

The primary aim of the Rapanui expedition, part of the "Tour du Monde" of the research vessel N/O *Jean Charcot*, was to collect detailed structural and geophysical data along the northern and southern Easter microplate boundaries, in order to test, in a rigorous manner, the proposed plate boundary configuration of Hey *et al.* (1985) and the most recent hypotheses concerning the kinematics of the microplate, including the instantaneous Nazca-Easter and Pacific-Easter Euler pole locations of Naar and Hey (1989) and the shear and rigid microplate models of Engeln *et al.* (1988) and Schouten *et al.* (1988a and b).

We have found that the configuration of the plate boundaries differs considerably from that suggested by Hey *et al.* (1985). The northern and southern boundaries are characterized by complex deformational structures, particularly at the northern and southern triple junctions. The northern boundary is dominated by compression and right lateral shear, particularly to the west, and leads to extension in the east. The southern boundary is dominated by extension, particularily to the west, leading to right lateral shear and compression to the east. The northern microplate boundary is characterized, from east to west, by a ridge-transform intersection, a short E-W strike-slip zone, a transform zone under the influence of compressional deformation, and a complex RFF (ridge-fault-fault) Pacific-Nazca-Easter triple junction region. The southern microplate boundary is characterized to the west by a large "V-shaped" (in plan view) ridge system, separating younger oceanic crust between the ridges from older oceanic crust to the north and south of the ridges. To the east this boundary is characterized by a low-relief, but tectonically complex, area containing a large overlapping spreading centre (OSC) and a RRF Pacific-Nazca-Easter triple junction. Although our detailed bathymetric data, as well as recent GLORIA data covering the Easter microplate (Searle *et al.*, 1989) may suggest that the NE and SW rifts are propagating rifts, additional constraints from magnetics over the length of the eastern and western microplate rifts will be needed to substantiate this.

We have found that our data agree fairly well with the Nazca-Easter and Pacific-Easter instantaneous Euler pole locations of Naar and Hey (1989). We have also found that our observations in general show agreement with the rigid microplate models of Engeln *et al.* (1988) and Schouten *et al.* (1988a and b), with the exception that the relative motion poles need not be located precisely on the plate boundaries, and appear to preclude the shear microplate model of Engeln *et al.* (1988). The indication from these models that the Easter microplate is *currently* behaving as a rigid plate (it may have had shear behaviour in the past), is in agreement with the findings of Naar and Hey (1989) that their three-plate-closure instantaneous Euler pole locations are closely coincident with their two plate pole locations.

Acknowledgements

We would like to thank R. Armijo and P. Tapponnier for fruitful discussions, and P. Patriat, B. de Ribet, and P. Slootweg for help in the laboratory during the course of this work. We are grateful to V. Marchig of BGR, Germany, and to the Scripps Institution of Oceanography for providing us with Seabeam data over the microplate. G. Aveline drafted the figures. We thank the officers and crew of the N/O *Jean Charcot*. IFREMER and INSU provided financial support for the Rapanui expedition.

REFERENCES

Anderson R. N., D. W. Forsyth, P. Molnar, J. Mammerickx (1974). Fault plane solutions of earthquakes on the Nazca plate boundaries and the Easter plate. *Earth Planet. Sci. Lett.*, **24**, 188-202.

Engeln J.F. (1985). Seismological studies of the tectonics of divergent plate boundaries, PhD thesis, Northwestern University.

Engeln J., S. Stein (1984). Tectonics of the Easter plate. *Earth Planet. Sci. Lett.*, **68**, 259-270.

Engeln J., S. Stein, J. Werner, R. Gordon (1988). Microplate and shear zone models for oceanic spreading center reorganizations, *J. Geophys. Res.*, **93**, 2839-2856.

Forsyth D.W. (1972). Mechanisms of eartquakes and plate motions in the east Pacific. *Earth Planet. Sci. Lett.*, **17**, 189-193.

Francheteau J., P. Patriat, S. Segoufin, R. Armijo, M. Doucoure, K. Yelles-Chaouche, J.H. Zukin, S. Calmant, D. Naar, R. Searle

(1988). Pito and Orongo fracture zones: the northern and southern boundaries of the Easter microplate (Southeast Pacific), *Earth Planet. Sci Lett.*, **17**, 189-193.

Handschumacher D. W., R.H. Pilger, J.A Foreman, J.F. Campbell (1981). Structure and evolution of the Easter plate. *GSA Memoir*, **154**, 63-76.

Herron E.M. (1972). Two small crustal plates in the south Pacific near Easter Island. *Nature Physical Science*, **240**, 35-37.

Hey R.N., D.F. Naar (1987). Cruise report, *R/V Moana Wave* 8711, 23pp.

Hey R. N., D. F. Naar, M.C. Kleinrock, W. J.P. Morgan, E. Morales, J.G. Schilling (1985). Microplate tectonics along a superfast seafloor spreading system near Easter Island. *Nature*, **317**, 320-325.

Le Pichon X., J. Francheteau, J. Bonnin (1973). Plate tectonics, Elsevier, Amsterdam, 300pp.

Mammerickx J., D. F. Naar, R. C.Tyce (1988). The mathematician palaeoplate. *J. Geophys. Res.*, **93**, 3025-3040.

Naar D. F., R. N. Hey (1986). Fast rift propagation along the East Pacific Rise near Easter Island; *J. Geophys. Res.*, **91**, 3425-3438.

Naar D.F., R.N.Hey (1989). Recent Pacific-Easter-Nazca plate motions, in: Evolution of mid ocean ridges, IUGG Symposium 8, *AGU Geophysical Monograph*, **57**, 9-30.

Parsons B., J.G. Sclater (1977). An analysis of the variation of ocean floor bathymetry and heat flow with age. *J. Geophys. Res.*,**82**, 803-827.

Renard V., J.P. Allenou (1979). Seabeam, Multi-beam echo-sounding in *Jean Charcot*; description, evaluation and first results. *International Hydrographic Review*, **56**, 1, 35-67.

Shouten H., K.D. Klitgord, D.G. Gallo (1988a). Microplate kinematics of the second order. (Submitted to *Nature*).

Shouten H., K.D. Klitgord, D.G. Gallo (1988b). Microplate kinematics of the second order. EOS, trans. American geophys. union, 69, 488.

Searle R.C, J. Engeln, R.N. Hey, J. Hoffman, P. Hunter, T. Le Bas, R. Livermore, R. Rusby, J.H. Zukin (1989). Comprehensive sonar imaging of the Easter microplate. *Nature*, **341**, 701-705.

Tisseau J., P. Patriat (1981). Identifications des anomalies magnétiques sur les dorsales à faible taux d'expansion : méthode des taux fictifs, *Earth Planet. Sci. Lett.*, **52**, 381-396.

Zukin J., J. Francheteau (1990). A tectonic study of the Easter microplate: the northern and southern boundaries, submitted to J. Geophys. Res.